Kumamoto University
Department of Electrical and Computer Engineering

Power System Stabiliser Design and Its Real-Time Implementation

HASSAN BEVRANI, TAKASHI HIYAMA

Technical Report (P04346)

April 2006

Abstract: This research work addresses a new robust control strategy to synthesis of robust proportional-integral-derivative (PID) based power system stabilizers (PSS). The PID based PSS design problem is reduced to find an optimal gain vector via an H∞ static output feedback control (H∞-SOF) technique, and the solution is easily carried out using a developed iterative linear matrix inequalities algorithm. To illustrate the developed approach a real-time experiment has been performed for a longitudinal four-machine infinite-bus system on the Analog Power System Simulator at the Research Laboratory of the Kyushu Electric Power Co. The results of the proposed control strategy are compared with full order H∞ and conventional PSS designs. The robust PSS is shown to maintain the robust performance and minimize the effect of disturbances properly.

Keywords: Power system stabilizer, PID, Static output feedback control, LMI, robust performance.

---

1 Introduction

The proportional-integral-derivative (PID) controller, because of its functional simplicity, is widely used in industrial applications. However, their parameters are often tuned using experiences or trial and error methods. Unfortunately, it has been quite difficult to tune properly the gains of PID controllers because many industrial systems are often burdened with problems such as structure complexity, uncertainties and nonlinearities.

Over the years, many different parameter tuning methods have been presented for PID controllers. A survey up to 2002 is given in Ref. [1-2]. Most of these methods present modifications of the frequency response method introduced by Ziegler and Nichols [3]. Some efforts have also been made to find analytical approaches to tune the parameters [4-6]. Several tuning methodology based on robust and optimal control techniques are introduced to design of PI/PID controllers [7-11].

In parallel with other industries, the PID controllers are commonly used in power systems control and operation. However, because of expanding physical steps, functionality and complexity of power systems, it is very difficult to maintain a desired performance for a wide range of operation using conventionally tuned PID based power system controllers. Although the most of recent addressed approaches introduce high-order control structure which have been proposed based on new contributions in modern control systems, because of complexity of control structure, numerous unknown design parameters and neglecting real constraints, they are not well suited to meet the design objectives in a real multi-machine power system.

Recently, some techniques have been proposed for tuning of PID based power system stabilisers (PSSs). Several self-tuning PID-PSSs were presented for improving the dynamic stability of single or multimachine power systems [12-14]. In [15-17], state space eigenvalue analysis is carried out to determine the stable operating gain regions for PI and PID controllers to stabilise of power systems. The IEEE working group publications [18-19] summarise generally accepted PID controller tuning guidelines in terms of generator parameters with margins for stability. Some fuzzy logic based PID-PSSs were proposed in [20-22]. [23, 24] used genetic algorithm (GA) to set the PID gains of a power

system stabiliser.

In the present work, the PID based PSS design problem is transferred to an H∞ static output feedback (H∞-SOF) control problem. The main merit of this transformation is in possibility of using the well-known SOF control techniques to calculate the fixed gains, and once the SOF gain vector is obtained, the PID gains are ready in hand and no additional computation is needed.

In a given PID-based control system *i*, the measured output signal (for example the speed deviation ω_i) performs the input signal for the controller and we can write

$$u_i = k_{Pi}\omega_i + k_{Ii}\int \omega_i + k_{Di}\frac{d\omega_i}{dt}. \qquad (1)$$

where k_{Pi}, k_{Ii} and k_{Di} are constant real numbers. In order to change (1) to a simple SOF control as $u_i = K_i y_i$, we can rewrite it as follows

$$u_i = [k_{Pi} \quad k_{Ii} \quad k_{Di}]\left[\omega_i \quad \int \omega_i \quad \frac{d\omega_i}{dt}\right]^T \qquad (2)$$

Therefore, by augmenting the power system description to include the ω_i, it's integral and derivative as a new measured output vector (y_i), the PID control problem becomes one of finding a static output feedback that satisfied prescribed performance requirements.

Finally, since the solution of resulted non convex inequalities using the general linear matrix inequalities (LMI) technique is not possible, to solve the H∞-SOF control problem and to obtain the optimal static gains (PID parameters), an iterative LMI algorithm is developed. The preliminary step of this work has been presented in [25].

The proposed controller uses the measurable signals and has merely proportional gains; so gives considerable promise for implementation, especially in a multi-machine system. In fact the proposed control strategy attempts to make a bridge between the simplicity of control structure (simple PID) and robustness of stability and performance (using H∞ theory) to satisfy the PSS tasks.

To demonstrate the efficiency of the proposed control method, a real time experience has been performed on a four-machine infinite-bus system using the large scale Analog Power System Simulator at the Research Laboratory of the Kyushu Electric Power Company (Japan). The obtained results are

compared with conventional and full order H∞ controllers. The robust PID based PSS is shown to maintain the robust performance and minimise the effect of disturbances properly.

2 Test System

The test system is a modified 12-bus, 4-machine model of the West Japan Power System. A single line representation of the study system is shown in Fig. 1. Although, in the given model the number of generators is reduced to four, it closely represents the dynamic behavior of the west part of the West Japan Power System, and it is widely used by Japanese researchers [26, 27, 28]. The most important global and local oscillation modes of actual system are included. Each unit is considered a thermal unit, and has a separately conventional excitation control system as shown in Figs. 2a and 2b.

Each unit has a full set of governor-turbine system (governor, steam valve servo-system, high-pressure turbine, intermediate-pressure turbine, and low-pressure turbine) which is shown in Fig. 3. The generators, lines, conventional excitation system and governor-turbine parameters are given in Table 1, Table 2, Table 3 and Table 4 (Appendix), respectively.

3 Power System Modeling

In order to design a robust power system controller, it is first necessary to consider an appropriate linear mathematical description of multi-machine power system with two axis generator models. In the view point of 'generator unit *i*', the state space representation model for such a system has the form

$$\begin{aligned}
\dot{x}_{1i} &= x_{2i} \\
\dot{x}_{2i} &= -(D_i/M_i)x_{2i} - (1/M_i)\Delta P_{ei}(x) \\
\dot{x}_{3i} &= -(1/T'_{d0i})x_{3i} - (\Delta x_{di}(x)/T'_{d0i})\Delta I_{di}(x) + u_i \\
\dot{x}_{4i} &= -(1/T'_{q0i})x_{4i} - (\Delta x_{qi}(x)/T'_{q0i})\Delta I_{qi}(x)
\end{aligned} \tag{3}$$

where the states

$$x_i^T = \begin{bmatrix} x_{1i} & x_{2i} & x_{3i} & x_{4i} \end{bmatrix} = \begin{bmatrix} \delta_i & \omega_i & E'_{qi} & E'_{di} \end{bmatrix} \tag{4}$$

are defined as deviation form the equilibrium values

$$x_{ei}^{T} = \begin{bmatrix} \delta_{1i}^{e} & \omega_{2i}^{e} & E_{qi}^{\prime e} & E_{di}^{\prime e} \end{bmatrix} \tag{5}$$

and, here

$$\Delta x_{di} = x_{di} - x_{di}^{\prime}, \ \Delta x_{qi} = x_{qi} - x_{di}^{\prime} \tag{6}$$

$$\Delta P_{ei}(x) = (E_{di}^{\prime} I_{di} + E_{qi}^{\prime} I_{qi}) - (E_{di}^{\prime e} I_{di}^{e} + E_{qi}^{\prime e} I_{qi}^{e}) \tag{7}$$

$$\begin{aligned} I_{di} = & \sum_{k} [G_{ik} \cos \delta_{ik} + B_{ik} \sin \delta_{ik}] E_{dk}^{\prime} \\ & + \sum_{k} [G_{ik} \sin \delta_{ik} - B_{ik} \cos \delta_{ik}] E_{qk}^{\prime} \end{aligned} \tag{8}$$

$$\begin{aligned} I_{qi} = & \sum_{k} [B_{ik} \cos \delta_{ik} - G_{ik} \sin \delta_{ik}] E_{dk}^{\prime} \\ & + \sum_{k} [G_{ik} \cos \delta_{ik} + B_{ik} \sin \delta_{ik}] E_{qk}^{\prime} \end{aligned} \tag{9}$$

A detailed description of all symbols and quantities can be found in [29]. Using the linearization technique and after some manipulation, the nonlinear state equations (3) can be expressed in the form of following linear state space model.

$$\dot{x}_i = A_i x_i + B_i u_i \tag{10}$$

where

$$A_i = \begin{bmatrix} 0 & 1 & 0 & 0 \\ a_{21} & -\dfrac{D_i}{M_i} & a_{23} & a_{24} \\ a_{31} & 0 & a_{33} & -\dfrac{G_{ii} \Delta x_{di}}{T_{d0i}^{\prime}} \\ a_{41} & 0 & \dfrac{G_{ii} \Delta x_{qi}}{T_{q0i}^{\prime}} & a_{44} \end{bmatrix}, B_i = \begin{bmatrix} 0 \\ 0 \\ 1 \\ \dfrac{1}{T_{d0i}^{\prime}} \\ 0 \end{bmatrix} \tag{11}$$

4 Proposed Control Strategy

4.1 H∞ SOF Design

This section gives a brief overview for the H∞ based static output feedback (H∞-SOF) control design. Consider a linear time invariant system $G(s)$ with the following state-space realization.

$$G_i(s):\begin{aligned}\dot{x}_i &= A_i x_i + B_{1i} w_i + B_{2i} u_i \\ z_i &= C_{1i} x_i + D_{12i} u_i \\ y_i &= C_{2i} x_i\end{aligned} \tag{12}$$

where x_i is the state variable vector, w_i is the disturbance and area interface vector, z_i is the controlled output vector and y_i is the measured output vector. The A_i, B_{1i}, B_{2i}, C_{1i}, C_{2i} and D_{12i} are known real matrices of appropriate dimensions.

The H∞-SOF control problem for the linear time invariant system $G_i(s)$ with the state-space realization of (12) is to find a gain matrix K_i ($u_i = K_i y_i$), such that the resulted closed-loop system is internally stable, and the H∞ norm from w_i to z_i (Fig. 4) is smaller than γ, a specified positive number, i.e.

$$\left\| T_{z_i w_i}(s) \right\|_\infty < \gamma \tag{13}$$

It is notable that the H∞-SOF control problem can be transferred to a generalized SOF stabilization problem which is expressed via the following theorem [30].

Theorem. The system (*A, B, C*) is stabilizable via SOF if and only if there exist *P>0*, *X>0* and K_i satisfying the following quadratic matrix inequality

$$\begin{bmatrix} A^T X + XA - PBB^T X - XBB^T P + PBB^T P & (B^T X + K_i C)^T \\ B^T X + K_i C & -I \end{bmatrix} < 0 \tag{14}$$

Here, the matrices *A*, *B* and *C* are constant and have appropriate dimensions. The *X* and *P* are symmetric and positive-definite matrices (Proof is given in [30]).

Since a solution for the consequent non convex optimisation problem (14) can not be directly achieved by using general LMI technique [31], a variety of methods were proposed by many researchers with many analytical and numerical methods to approach a local/global solution. In Section 4.3, to solve the resulted SOF problem, an iterative LMI is introduced based on the existence necessary and sufficient condition for SOF stabilisation, via the H∞ control technique.

4.2 Control Framework

The overall control structure using SOF control design for an assumed power system is shown in Fig. 5, where Δv_{refi} and d_i show the reference voltage deviation and system disturbance input, respectively.

Using the linearized model for a given power system "*i*" in the form of (12) and performing the standard H∞-SOF configuration (Fig. 4) with considering an appropriate controlled output signals results an effective control framework. This control structure adapts the H∞-SOF control technique with the described power system control targets and allows direct trade-off between robust performance and robust stability by merely tuning of a vector gain.

Here, disturbance input vector w_i, controlled output vector z_i and measured output vector y_i are considered as follows:

$$w_i^T = \begin{bmatrix} \Delta v_{refi} & d_i \end{bmatrix} \tag{15}$$

$$z_i^T = [\eta_{1i} v_{ti} \quad \eta_{2i} \delta_i \quad \eta_{3i} u_i] \tag{16}$$

$$y_i^T = \begin{bmatrix} \omega_i & \int \omega_i & \dfrac{d\omega_i}{dt} \end{bmatrix} \tag{17}$$

where the ω_i and δ_i are the speed and rotor angle deviations. The η_{1i}, η_{2i} and η_{3i} are constant weights that must be chosen by designer to get the desired closed-loop performance. The selection of performance constant weights η_{1i} and η_{2i} is dependent on the specified voltage regulation and damping performance goals. In fact an important issue with regard to selection of these weights is the degree to which they can guarantee the satisfaction of design performance objectives.

Furthermore, η_{3i} sets a limit on the allowed control signal to penalize fast changes, large overshoot

with a reasonable control gain to meet the feasibility and the corresponded physical constraints. Since the vector z_i properly covers all significant controlled signals which must be minimized by an ideal PSS design, it is expected that the proposed robust controller could be able to satisfy the voltage regulation and stabilizing objectives, simultaneously. It is notable that, since the solution must be obtained trough the minimizing of an H∞ optimization problem, the designed feedback system satisfies the robust stability and robust performance for the overall closed-loop system. Moreover, the developed iterative LMI algorithm (which is described in the next section) provides an effective and flexible tool to find an appropriate solution in the form of a simple static gain controller.

4.3 Developed ILMI Algorithm

In order to solve the H∞-SOF, an iterative LMI algorithm has been used. The key point is to formulate the H∞ problem via a generalized static output stabilization feedback such that all eigenvalues of (A-$B K_i C$) shift towards the left half plane in the complex s-plane, to close to feasibility of (14). The described theorem in the previous section gives a family of internally stabilizing SOF gains is defined as K_{sof}. The desirable solution K_i is an admissible SOF law

$$u_i = K_i y_i \ , \ K_i \in K_{sof} \tag{18}$$

such that

$$\left\| T_{zi\,wi}(s) \right\|_\infty < \gamma^* , \ \left| \gamma - \gamma^* \right| < \varepsilon \tag{19}$$

where ε is a small positive number. The performance index γ^* indicates a lower bound such that the closed-loop system is H∞ stabilizable. The optimal performance index (γ), can be obtained from the application of a full dynamic H∞ dynamic output feedback control method.

The proposed algorithm, which gives an iterative LMI solution for above optimization problem, includes the following steps:

Step 1. Set initial values and compute the new (generalized) system (A_g, B_g, C_g) for the given power system (12) as follows:

$$A_g = \begin{bmatrix} A_i & B_{1i} & 0 \\ 0 & -\gamma I/2 & 0 \\ C_{1i} & 0 & -\gamma I/2 \end{bmatrix},\ B_g = \begin{bmatrix} B_{2i} \\ 0 \\ D_{12i} \end{bmatrix},\ C_g = \begin{bmatrix} C_{2i} & 0 & 0 \end{bmatrix} \tag{20}$$

Step 2. Set $i = 1$, $\Delta\gamma = \Delta\gamma_0$ and let $\gamma_i = \gamma_0 > \gamma$. $\Delta\gamma_0$ and γ_0 are positive real numbers.

Step 3. Select $Q > 0$, and solve $\overline{X}$ from the following algebraic Riccati equation

$$A_g{}^T \overline{X} + \overline{X} A_g - \overline{X} B_g B_g{}^T \overline{X} + Q = 0 \tag{21}$$

Set $P_1 = \overline{X}$.

Step 4. Solve the following optimization problem for $\overline{X}_i$, K_i and a_i.

Minimize a_i subject to the LMI constraints:

$$\begin{bmatrix} A_g{}^T \overline{X}_i + \overline{X}_i A_g - P_i B_g B_g{}^T \overline{X}_i - \overline{X}_i B_g B_g{}^T P_i + P_i B_g B_g{}^T P_i - a_i \overline{X}_i & (B_g{}^T \overline{X}_i + K_i C_g)^T \\ B_g{}^T \overline{X}_i + K_i C_g & -I \end{bmatrix} < 0 \tag{22}$$

$$\overline{X}_i = \overline{X}_i^T > 0. \tag{23}$$

Denote a_i^* as the minimized value of a_i.

Step 5. If $a_i^* \le 0$, go to step 8.

Step 6. For $i > 1$, if $a_{i-1}^* \le 0$, $K_{i-1} \in K_{sof}$ is an H∞ controller and $\gamma^* = \gamma_i + \Delta\gamma$ indicates a lower bound such that the above system is H∞ stabilizable via SOF control. Go to step 10.

Step 7. If $i = 1$, solve the following optimization problem for $\overline{X}_i$ and K_i:

Minimize trace($\overline{X}_i$) subject to the above LMI constraints (22-23) with $a_i = a_i^*$. Denote $\overline{X}_i^*$ as the $\overline{X}_i$ that minimized trace($\overline{X}_i$).Go to step 9.

Step 8. Set $\gamma_i = \gamma_i - \Delta\gamma$, $i = i+1$. Then do steps 3 to 5.

Step 9. Set $i = i+1$ and $P_i = \overline{X}^*_{i-1}$, then go to step 4.

Step 10. If the obtained solution (K_{i-1}) satisfies the gain constraint, it is desirable, otherwise retune constant weights (η_i) and go to step 1.

The proposed iterative LMI algorithm shows that if we simply perturb A_g to $A_g - (a/2)I$ for some $a > 0$, then we will find a solution of the matrix inequality (12) for the performed generalized plant. That is, there exist a real number ($a > 0$) and a matrix P>0 to satisfy inequality (22). Consequently, the closed-loop system matrix $A_g - B_g K C_g$ has eigenvalues on the left-hand side of the line $\Re(s) = a$ in the complex s-plane. Based on the idea that all eigenvalues of $A_g - B_g K C_g$ are shifted progressively towards the left half plane through the reduction of a. The given generalized eigenvalue minimization in the developed iterative LMI algorithm guarantees this progressive reduction.

5 Real Time Implementation

To illustrate the effectiveness of the proposed control strategy, a real time experiment has been performed on the large scale Analog Power System Simulator at the Research Laboratory of the Kyushu Electric Power Company. The whole power system (shown in Fig. 1) has been implemented in the mentioned laboratory. Fig. 6 shows the overview of the applied laboratory experiment devices including the hardware and control/monitoring desk.

Unit 1 is selected to be equipped with robust PID control, and therefore our objective is to apply the control strategy described in the previous section to controller design for unit 1. Using the described control methodology in section 4, a set of optimal PID parameters for the problem at hand is obtained as follows.

$$K_{PID} = [k_P \quad k_I \quad k_D] = [0.9615 \quad 0.5308 \quad 0.2140] \tag{24}$$

The proposed PID control loop has been built in a personal computer were connected to the power system using a digital signal processing (DSP) board equipped with analog to digital (A/D) and digital to analog (D/A) converters as the physical interfaces between the personal computer and the analog power system hardware. In order to signal conditioning, the input/output scaling blocks are used to match the PC based controller and the Analog Power System hardware, and, high frequency noises are removed by appropriate low pass filters.

The considered constraints on limiters and control loop gains are set according to the real power system control units and close to ones that exist for the conventional PSS unit. The used constant weight vector (η_i) is given in Appendix.

6. Experiment Results

The performance of the proposed robust PID (RPID) controller when a voltage deviation, fault and system disturbance is injected into the interconnected system is studied, and, the controller is compared with a conventional PSS (CPSS). The configuration of the applied CPSS that was accurately tuned by the expert operators (who have worked on the system for the several past years), is illustrated in Fig. 7. Furthermore, to provide a comparison of what is lost in performance using the simple PID controller over a high order controller to achieve the same purpose, an H∞ controller [32] is applied and its performance is compared with the RPID controller.

Fig. 8 shows the electrical power of all units, with the terminal voltage and machine speed of unit 1, following a fault on the line between buses 11 and 12 at 2 sec. It can be seen that in comparison of CPPS, the system response is quite improved using the designed RPID controller. Fig. 8 shows that although the proposed PID controller has a very simple structure, however it is able to maintain the robust performance as well as full order H∞ controller.

Furthermore, the size of resulted stable region by the proposed method is significantly enlarged in comparison of CPSS controller. To show this fact, the critical power output from unit 1 in the presence of a three-phase to ground fault is considered as a measure tool. To investigate the critical point, the real power output of unit 1 is increased from 0.1 pu (The setting of the real power output from the other units is fixed at the values shown in Fig. 1). Using the CPSS structure, the resulted critical power output from unit 1 to be 0.31 pu [27, 28]; and in case of tight tuning of CPSS parameters (similar to the performed experiment in the present work) it could not be higher than 0.52 pu. The critical power output for the applied three PSS is

given in Table 5. It can be seen that the simple PID controller designed by this method has a stability margin that is comparable to the more complex H∞ controller. During the test scenarios appeared in this paper, the output setting of unit 1 is fixed to 0.4 pu.

In the second test case, the performance of designed controllers was evaluated in the presence of a 0.05 pu step disturbance injected at the voltage reference input of unit 1 at 20 sec. Fig. 9 shows the closed-loop response of the power systems fitted with the CPSS, H∞ and the proposed RPID controllers. In comparison of CPSS, the better performance is achieved by the developed control strategy.

Finally, the system response in the face of a step disturbance (*d*) in the closed-loop system at 20 sec, is shown in Fig. 10. Comparing the experiment results shows that the robust design achieves robustness against the voltage deviation, disturbance and line fault with a quite good damping performance.

7. Conclusion

In this work, to provide robust performance and stability over a wide range of power system operating points, a new tuning methodology has been proposed for robust PID based power system stabilizers. For this purpose, a control strategy is developed using H∞-SOF control technique via an iterative LMI algorithm. The proposed method was applied to a four-machine infinite bus power system, through a real-time experiment, and the results are compared with conventional PSS and complex H∞ control designs. The performance of the resulting closed-loop system is shown to be satisfactory over a wide range of operating conditions.

As shown in the performed real-time laboratory experiments, the proposed robust PID control loop has brought a significant effect to improve the power system performance and to widen the stable region. It has been shown that the simple PID controller designed by this method has a performance and robust stability that is comparable the more complex H∞ controller. Furthermore, because of simplicity of structure, decentralized property, ease of formulation and flexibility of design methodology, it is practically desirable.

Acknowledgments

This work is supported in part by Japan Society for the Promotion of Science (JSPS) under grant P04346 and the Research Office at the University of Kurdistan. The authors would like to thank N. Wakasugi, A. Matsunaga, Y. Fujimoto, T. Kouichi, Y. Hirofumi and K. Hiroyuki for their helps to make a successful experiment in Research Laboratory of the Kyushu Electric Power Company.

References

[1] K. J. Astrom, T. Hagglund, C. C. Hang and W. K. Ho, Automatic tuning and adaptation for PID controllers – a survey, Control Eng. Pract., 1 (1993) 699-714.
[2] P. Cominos and N. Munro, PID controllers: recent tuning methods and design to specification, IEE Proc. Control Theory Appl., 149(1) (2002) 46-53.
[3] J. G. Ziegler and N. B. Nichols, Optimum setting for automatic controllers, Trans. ASME, 64 (11) (1942) 759-765.
[4] W. K. Ho, C. C. Hang and L. S. Cao, Tuning of PID controllers based on gain and phase margin specifications, Automatica, 31(3) (1995) 497-502.
[5] A. J. Isakson and S. F. Graebe, Analytical PID parameter expressions for higher order systems, Automatica, 35 (6) (1999) 1121-1130.
[6] S. Skogestad, Simple analytic rules for model reduction and PID controller tuning, Journal of Process Control, 13 (2003) 291-309.
[7] B. Kristiansson and B. Lennartson, Robust and optimal tuning of PI and PID controllers, IEE Proc. On Control Theory and Applications, 149 (1) (2002) 17-25.
[8] E. Grassi, K. Tsakalis, S. Dash, S. V. Gaikwad, W. Macarthur and G. Stein, Integrated system identification and PID controller tuning by frequency loop-shaping, IEEE Trans. Control Syst. Technology, 9 (2) (2001) 285-294.
[9] C. Lin, Q. G. Wang and T. H. Lee, An improvement on multivariable PID controller design via iterative LMI approach, Automatica, 40 (2004) 519-525.
[10] F. Zheng, Q. G. Wang and T. H. Lee, On the design of multivariable PID controllers via LMI approach, Automatica, 38 (2002) 517-526.
[11] M. T. Ho, Synthesis of H∞ PID controllers: a parametric approach, Automatica, 39 (2003) 1069-1075.
[12] C. J. Wu and Y. Y. Hsu, Self-tuning excitation control for synchronous machine, IEEE Trans. AES, 22 (1986) 389-394.
[13] C. J. Wu and Y. Y. Hsu, Design of self-tuning power system stabilizer for multimachine power systems, IEEE Trans. Power Systems, 3 (3) (1988) 1059-1063.
[14] S. Cheng, O. P. Malik and G. S. Hope, Design of self-tuning PID stabilizer for a multimachine power system, IEE Proceedings- Part C, 133(4) (1986) 176-185.
[15] D. H. Thrne and E. F. Hill, Field testing and simulation of hydraulic turbine governor performance, IEEE Trans. Power App. Syst., PAS-93 (4) (1974) 1183-118.
[16] D. H. Thrne and E. F. Hill, Extensions of stability boundaries of a hydrolic turbine generating unit, IEEE Trans. Power App. Syst., PAS-94 (4) (1975) 1401-1408.
[17] D. T. Phi, E. J. Bourque, D. H. Thorme and E. F. Hill, Analysis and application of stability limits of a hydro-generating unit, IEEE Trans. Power App. Syst., PAS-100 (7) (1981) 3203-3211.
[18] IEEE Committee Report, Dynamic models for steam and hydro turbines in power system studies, IEEE Trans. Power App. Syst., PAS-92 (6) (1973) 1904-1915.

[19] IEEE Working Group on Prime Mover and Energy Supply Models for System Dynamic performance Studies, Hydraulic turbine and turbine control models for system dynamic studies, IEEE Trans. Power Syst., 7 (1) (1992) 167-179.
[20] T. Hiyama and T. Fujiki, Fuzzy logic power system stabilizer using PID information of generator speed, IEEJ Trans. Power and Energy, 113 (12) (1993) 1353-1361.
[21] T. Hiyama, M. kugimiya and H. Satoh, "Advanced PID type fuzzy logic power system stabilizer," IEEE Trans. Energy Conversion, 9(3) (1994) 514-520.
[22] F. Mrad, S. Karaki and B. Copti, An adaptive Fuzzy-synchronous machine stabilizer, IEEE Trans. System Man and Cybernetics- Part C, 30 (1) (2000) 131-137.
[23] Y. P. Wang, N. R. Watson and H. H. Chong, Modified genetic algorithm to design of an optimal PID controller for AC-DC transmission systems, Int. journal of Electrical Power and Energy Systems, 24 (2002) 59-69.
[24] P. Bera, D. Das and T. K. Basu, design of PID power system stabilizer for multimachine system, in Proc. of IEEE India Annual Conf. (INDCON), 2004, pp. 446-450.
[25] H. Bevrani, T. Hiyama, Stability and voltage regulation enhancement using an optimal gain vector, in Proc. of IEEE PES General Meeting, 2006, pp. 1-6, Canada.
[26] T. Hiyama, M. Kawakita, H. Ono, Multi-agent based wide area stabilization control of power systems using power system stabilizer, in Proc. of IEEE Int Conf on Power System Technology, 2004.
[27] T. Hiyama, D. Kojima, K. Ohtsu and K. Furukawa, Eigenvalue-based wide area stability monitoring of power systems, Control Engineering Practice, 13 (2005) 1515-1523.
[28] T. Hiyama, S. Oniki and H. Nagashima, Evaluation of advanced fuzzy logic PSS on analog network simulator and actual installation on hydro generators, IEEE Trans on Energy Conversion, 11(1) (1996) pp. 125-131.
[29] P. W. Sauer and M. A. Pai, Power system dynamic and stability, Englewood Cliffs, NJ; Prentice-Hall, 1998.
[30] Y. Y. Cao, J. Lam, Y. X. Sun and W. J. Mao, Static output feedback stabilization: an ILMI approach, Automatica, 34 (12) (1998) 1641-1645.
[31] S. P. Boyed, L. El Chaoui, E. Feron and V. Balakrishnan, Linear matrix inequalities in systems and control theory, Philadelphia, PA: SIAMA, 1994.
[32] H. Bevrani and T. Hiyama, Robust design of power system stabilizer: an LMI approach, In Proc. of IASTED Int. Conf. on Energy and Power Systems (CD ROM), 2006, Chiang Mai, Thailand.

Appendix

The elements of A_i matrix in (11):

$$a_{21} = -\frac{1}{M_i}\frac{\partial f_{1i}(x)}{\partial x_{1i}}\bigg|_{x_{ei}}$$

$$a_{23} = -\frac{\left[G_{ii}E'^{e}_{qi} - B_{ii}E'^{e}_{di} + I^{e}_{qi}\right]}{M_i} - \frac{1}{M_i}\frac{\partial f_{1i}(x)}{\partial x_{3i}}\bigg|_{x_{ei}}$$

$$a_{24} = -\frac{\left[G_{ii}E'^{e}_{di} + B_{ii}E'^{e}_{qi} + I^{e}_{di}\right]}{M_i} - \frac{1}{M_i}\frac{\partial f_{1i}(x)}{\partial x_{4i}}\bigg|_{x_{ei}}$$

$$a_{31} = -\frac{\Delta x_{di}}{T'_{d0i}}\frac{\partial f_{2i}(x)}{\partial x_{1i}}\bigg|_{x_{ei}},\ a_{33} = -\frac{1}{T'_{d0i}} + \frac{B_{ii}\Delta x_{di}}{T'_{d0i}}$$

$$a_{41} = -\frac{\Delta x_{qi}}{T'_{q0i}}\frac{\partial f_{3i}(x)}{\partial x_{1i}}\bigg|_{x_{ei}},\ a_{44} = -\frac{1}{T'_{q0i}} + \frac{B_{ii}\Delta x_{qi}}{T'_{q0i}}$$

where

$$f_{1i}(x) = x_{4i}\Delta I_{di}(x) + x_{3i}\Delta I_{qi}(x) + \sum_{k\neq i}\Big\{[E'^{e}_{di}\eta_{ik}(\delta) + E'^{e}_{qi}\hat{\eta}_{ik}(\delta)]x_{4k}$$
$$+[E'^{e}_{di}\nu_{ik}(\delta) + E'^{e}_{qi}\hat{\nu}_{ik}(\delta)]x_{3k} + [E'^{e}_{di}\upsilon_{ik}(\delta) + E'^{e}_{qi}\hat{\upsilon}_{ik}(\delta)]\sin\phi_{ik}\Big\}$$

$$f_{2i}(x) = \sum_{k\neq i}\left[\eta_{ik}(\delta)x_{4k} + \nu_{ik}(\delta)x_{3k} + \upsilon_{ik}(\delta)\sin\phi_{ik}\right]$$

$$f_{3i}(x) = \sum_{k\neq i}\left[\hat{\eta}_{ik}(\delta)x_{4k} + \hat{\nu}_{ik}(\delta)x_{3k} + \hat{\upsilon}_{ik}(\delta)\sin\phi_{ik}\right]$$

$$\eta_{ik}(\delta) = G_{ik}\cos\delta_{ik} + B_{ik}\sin\delta_{ik},\ \hat{\eta}_{ik}(\delta) = B_{ik}\cos\delta_{ik} - G_{ik}\sin\delta_{ik}$$

$$\nu_{ik}(\delta) = G_{ik}\sin\delta_{ik} - B_{ik}\cos\delta_{ik},\ \hat{\nu}_{ik}(\delta) = B_{ik}\sin\delta_{ik} - G_{ik}\cos\delta_{ik}$$

$$\upsilon_{ik}(\delta) = 2g1_{ik}\sin\frac{\delta^e_{ik}+\delta_{ik}}{2} + 2g2_{ik}\cos\frac{\delta^e_{ik}+\delta_{ik}}{2},\ \phi_{ik} = 0.5(x_{1i}-x_{1k})$$

$$\hat{\upsilon}_{ik}(\delta) = 2g2_{ik}\sin\frac{\delta^e_{ik}+\delta_{ik}}{2} - 2g1_{ik}\cos\frac{\delta^e_{ik}+\delta_{ik}}{2},\ \ \delta_{ik} = \delta_i - \delta_k$$

$$g1_{ik} = G_{ik}E'^e_{dk} - B_{ik}E'^e_{qk},\ \ g2_{ik} = G_{ik}E'^e_{qk} + B_{ik}E'^e_{qk}$$

Constant weights: $\eta_1 = [0.80 \quad 0.25 \quad 10]$

Figure Captions

Figure 1. Four-machine infinite-bus power system

Figure 2. Conventional excitation control system; a) for units 2 and 3, b) for units 1 and 4

Figure 3. a) Conventional speed governing system, b) Detailed turbine system

Figure 4. Closed-loop system via H∞-SOF control

Figure 5. The proposed control framework

Figure 6. Performed laboratory experiment

Figure 7. Conventional power system stabilizer

Figure 8. System response for a fault between buses 11 and 12, while the output setting of unit 1 is fixed to 0.4 pu.; Solid (RPID), dash-dotted (H∞), dotted (CPSS)

Figure 9. System response for a 0.05 pu step change at the voltage reference input of unit 1; Solid (RPID), dash-dotted (H∞), dotted (CPSS)

Figure 10. System response for a step disturbance at 20 sec; Solid (RPID), dash-dotted (H∞), dotted (CPSS)

Tables

Table 1. Generator constants

Unit No.	M_i (sec)	D_i	x_{di} (pu)	x'_{di} (pu)	x_{qi} (pu)	x'_{qi} (pu)	T'_{d0i} (sec)	T'_{q0i} (sec)	MVA
1	8.05	0.002	1.860	0.440	1.350	1.340	0.733	0.0873	1000
2	7.00	0.002	1.490	0.252	0.822	0.821	1.500	0.1270	600
3	6.00	0.002	1.485	0.509	1.420	1.410	1.550	0.2675	1000
4	8.05	0.002	1.860	0.440	1.350	1.340	0.733	0.0873	900

Table 2. Line parameters

Line No.	*Bus-Bus*	R_{ij} (pu)	X_{ij} (pu)	S_{ij} (pu)
1	1-9	0.02700	0.1304	0.0000
2	2-10	0.07000	0.1701	0.0000
3	3-11	0.04400	0.1718	0.0000
4	4-12	0.02700	0.1288	0.0000
5	10-6	0.02700	0.2238	0.0000
6	11-7	0.04000	0.1718	0.0000
7	12-8	0.06130	0.2535	0.0000
8	9-10	0.01101	0.0829	0.0246
9	10-11	0.01101	0.0829	0.0246
10	11-12	0.01468	0.1105	0.0328
11	12-5	0.12480	0.9085	0.1640

Table 3. Excitation parameters

K_1	K_2	K_3	K_4	$\lvert E_{max(min)} \rvert$	U_{max}	U_{min}
1.00	19.21	10.00	6.48	5.71	7.60	-5.20
T_1 (sec)	T_2 (sec)	T_3 (sec)	T_4 (sec)	T_5 (sec)	T_6 (sec)	T_7 (s)
0.010	1.560	0.013	0.013	0.200	3.000	10.000

Table 4. Governor and turbine parameters

Parameters	Unit 1	Unit 2	Unit 3	Unit 4
T_1 (Sec)	0.08	0.06	0.07	0.07
T_2 (Sec)	0.10	0.10	0.10	0.10
T_3 (Sec)	0.10	0.10	0.10	0.10
T_4 (Sec)	0.40	0.36	0.42	0.42
T_5 (Sec)	10.0	10.0	10.0	10.0
T_H (Sec)	0.05	0.05	0.05	0.05
T_I (Sec)	0.08	0.08	0.08	0.08
T_L (Sec)	0.58	0.58	0.58	0.58
K_H (pu)	0.31	0.31	0.31	0.31
K_I (pu)	0.24	0.24	0.24	0.24
K_L (pu)	0.45	0.45	0.45	0.45
M_1 (pu/Minute)	0.50	0.50	0.50	0.50
M_2 (pu/Minute)	0.20	0.20	0.20	0.20
M_3 (pu/Minute)	1.50	1.50	1.50	1.50
N_1 (pu/Minute)	-0.50	-0.50	-0.50	-0.50
N_2 (pu/Minute)	-0.20	-0.20	-0.20	-0.20
N_3 (pu/Minute)	-0.50	-0.50	-0.50	-0.50

Table 5. Critical power output of Unit 1

Control design	*Critical power output*
RPID	*0.94* (*pu*)
CPSS	*0.52* (*pu*)
H∞	*0.96* (*pu*)

Figures

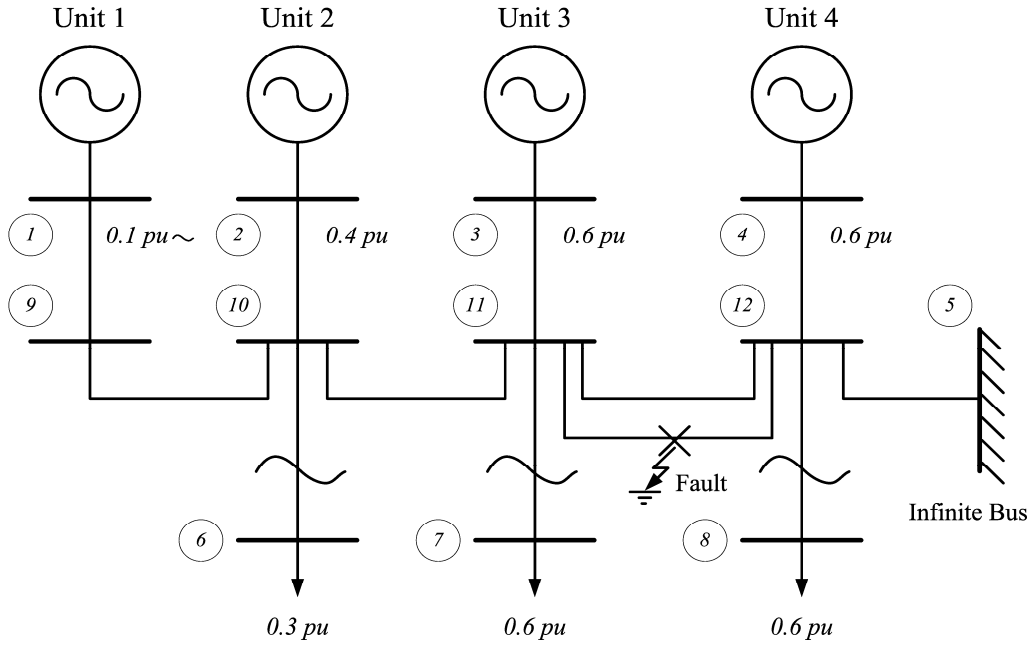

Figure 1. Four-machine infinite-bus power system

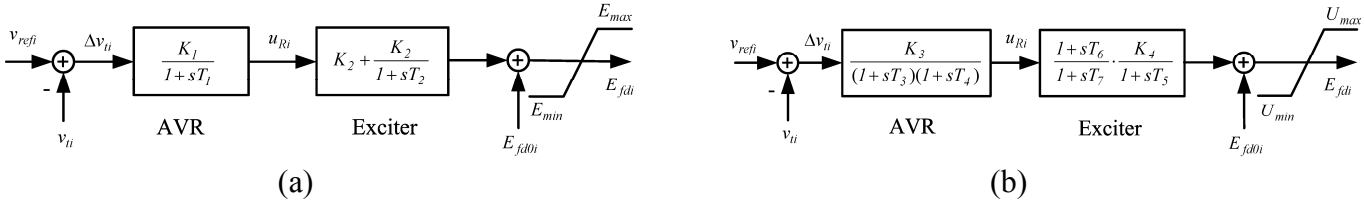

Figure 2. Conventional excitation control system; a) for units 2 and 3, b) for units 1 and 4.

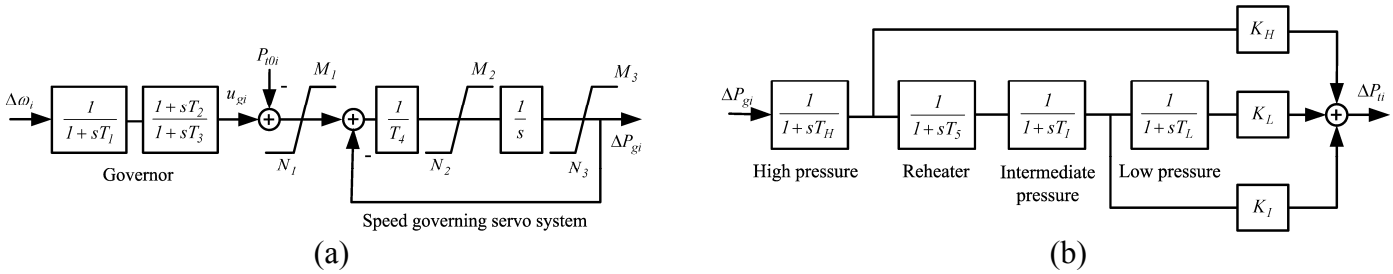

Figure 3. a) Conventional speed governing system, b) Detailed turbine system

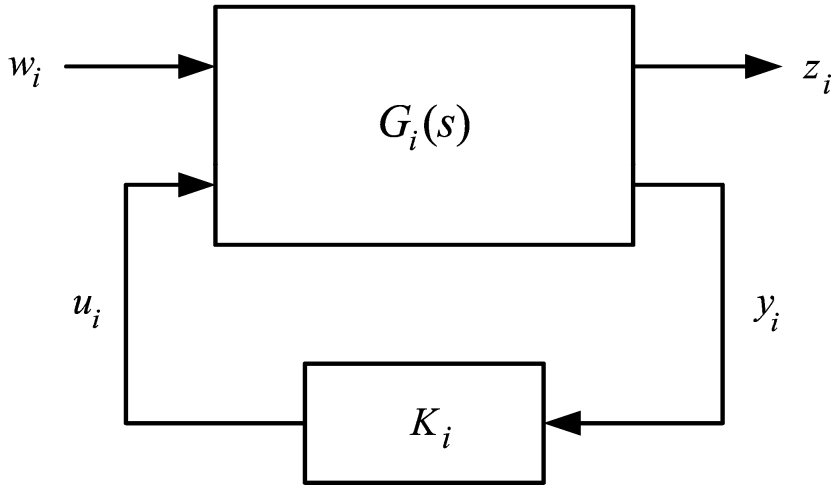

Figure 4. Closed-loop system via H∞-SOF control

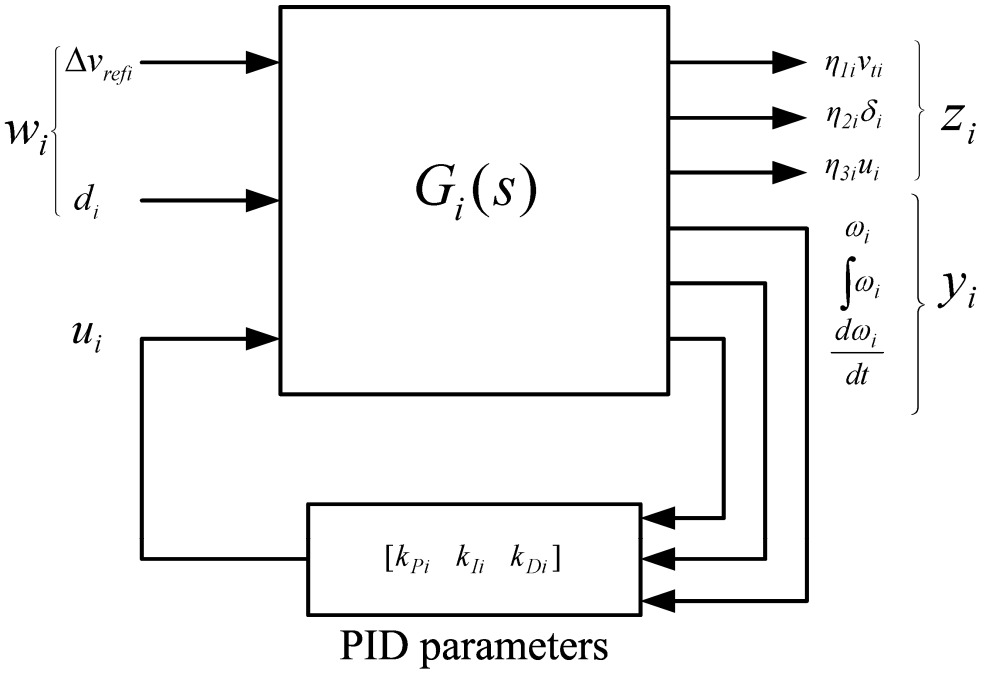

Figure 5. The proposed control framework

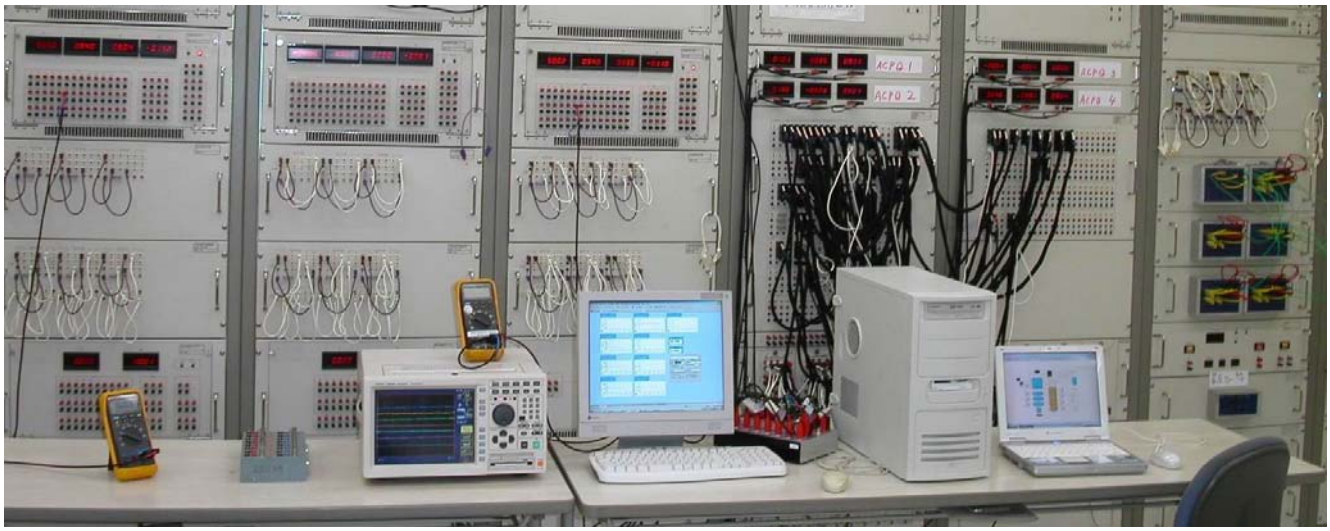

Figure 6. Performed laboratory experiment.

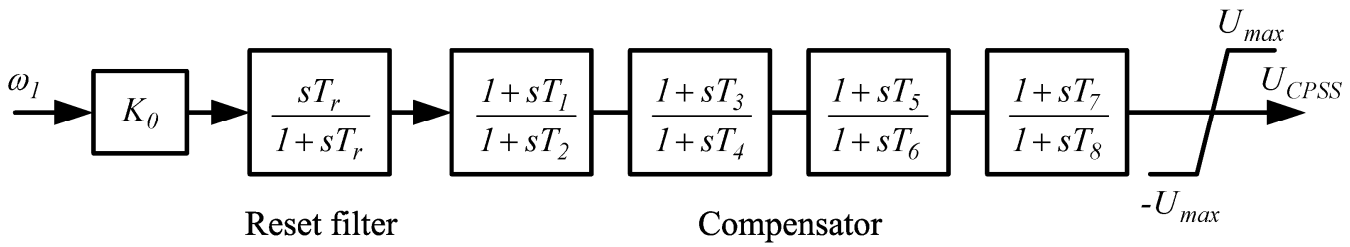

Figure 7. Conventional power system stabilizer

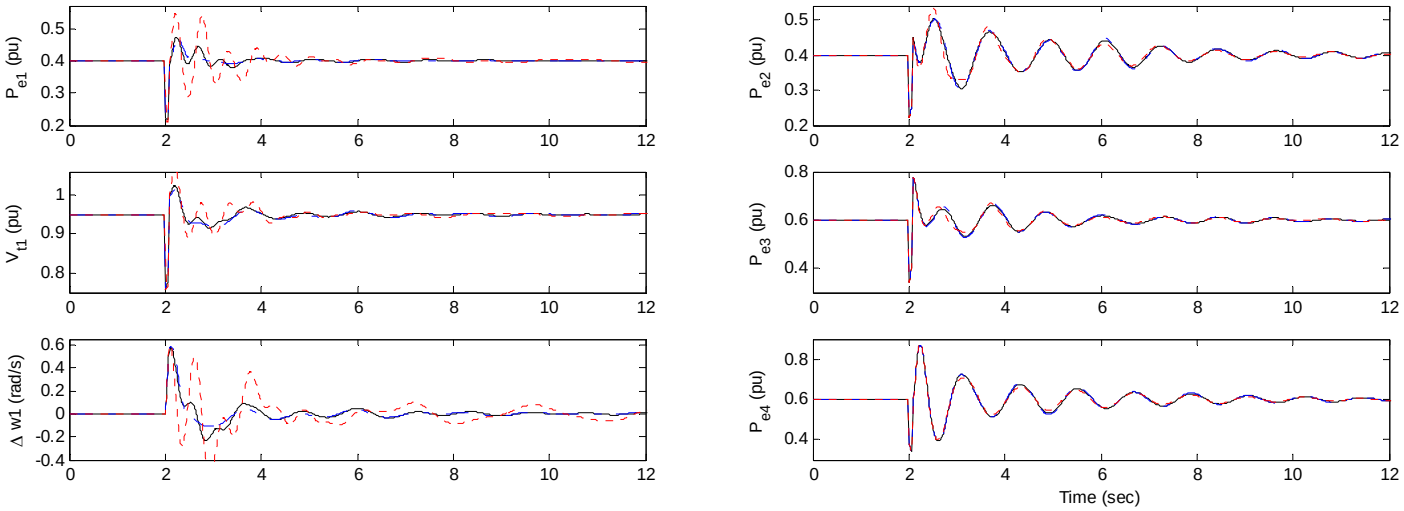

Figure 8. System response for a fault between buses 11 and 12, while the output setting of unit 1 is fixed to 0.4 pu.; Solid (RPID), dash-dotted (H∞), dotted (CPSS)

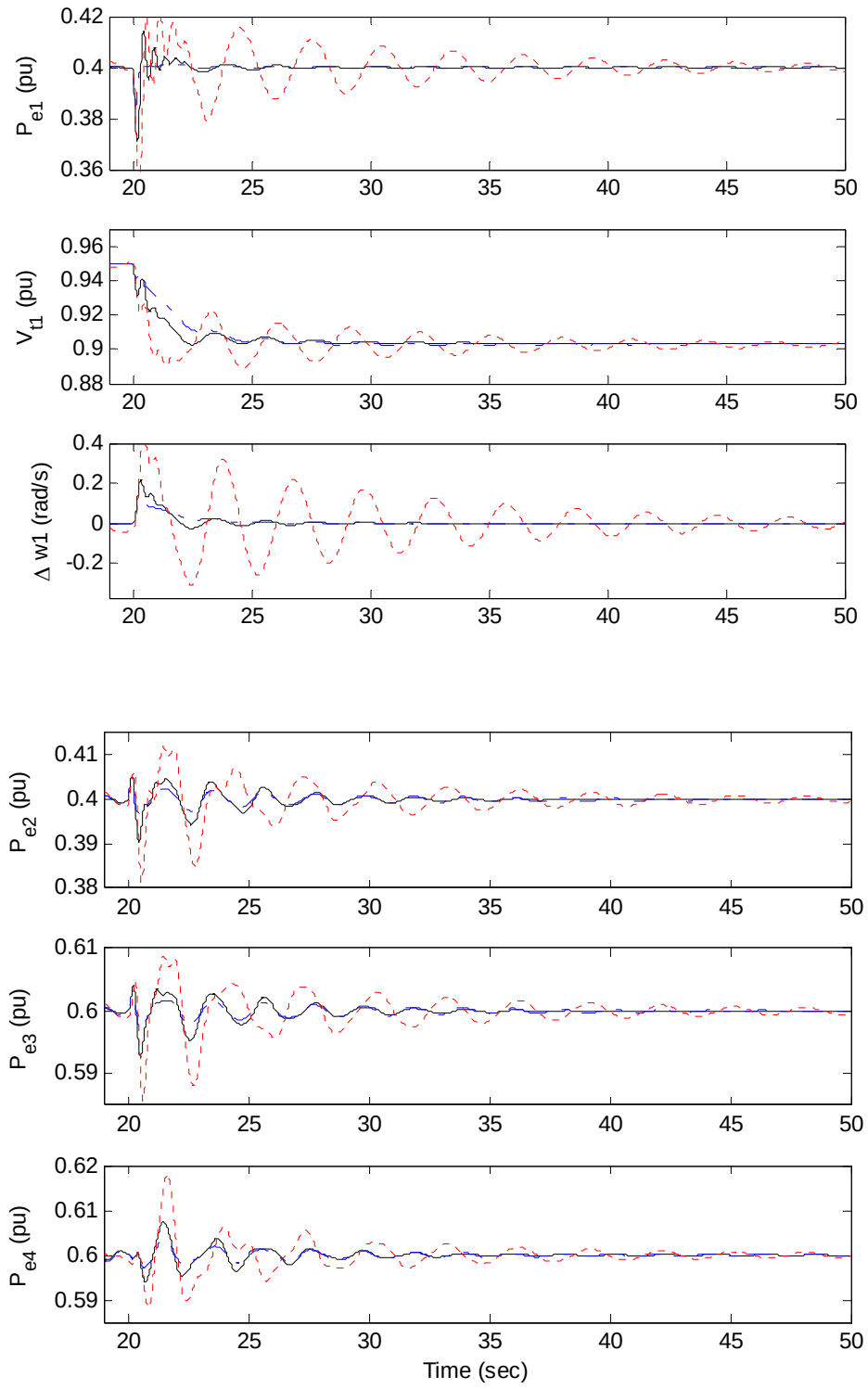

Figure 9. System response for a 0.05 pu step change at the voltage reference input of unit 1; Solid (RPID), dash-dotted (H∞), dotted (CPSS)

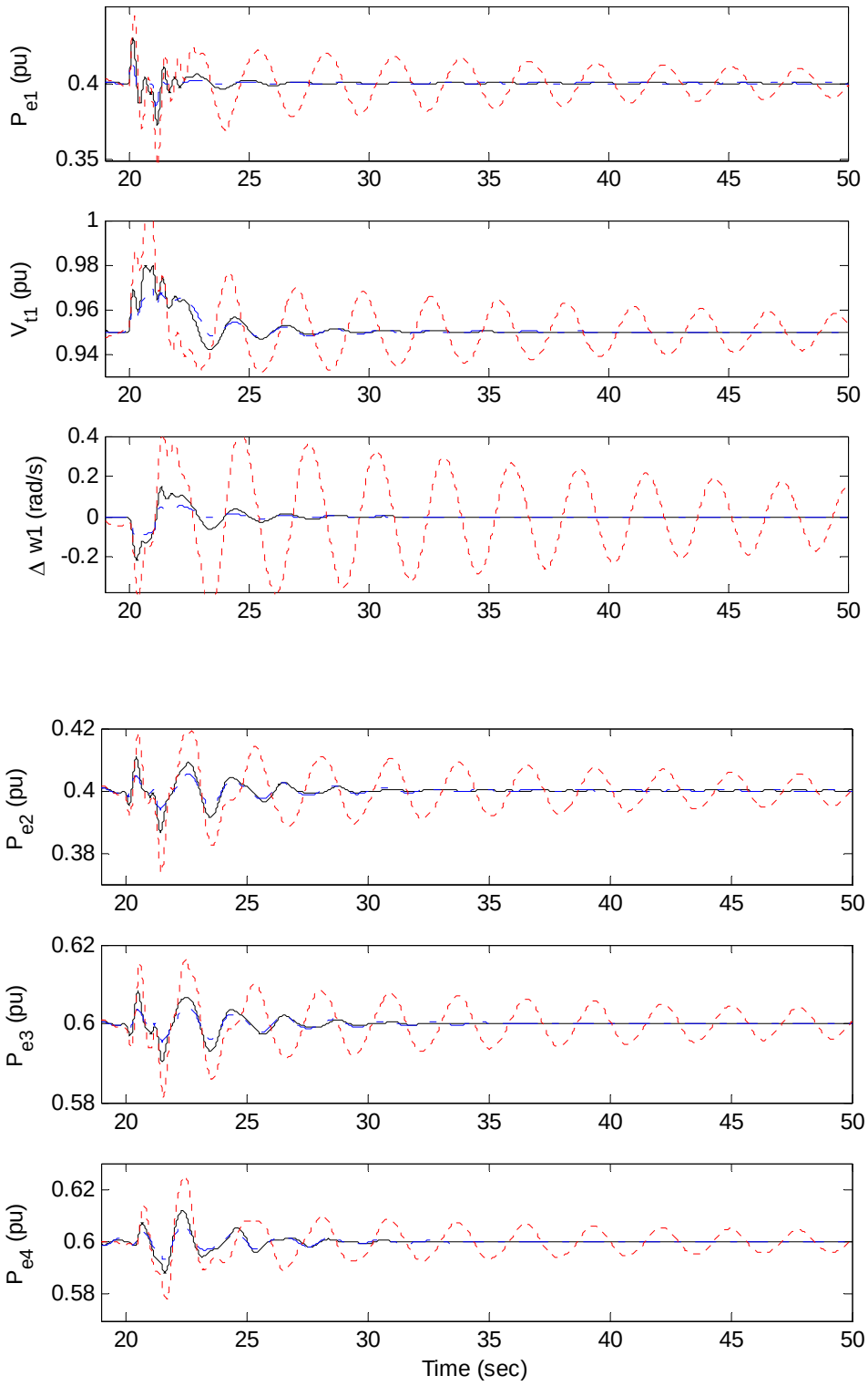

Figure 10. System response for a step disturbance at 20 sec; Solid (RPID), dash-dotted (H∞), dotted (CPSS)